

# Asymmetric Deep Semantic Quantization for Image Retrieval

ZHAN YANG<sup>1</sup>, OSOLO IAN RAYMOND<sup>1</sup>, WUQING SUN<sup>1</sup>, JUN LONG<sup>1,2\*</sup>

<sup>†1</sup>School of Computer Science and Engineering, Central South University, Changsha 410083, China

<sup>2</sup>Network Resources Management and Trust Evaluation Key Laboratory of Hunan Province

junlong@csu.edu.cn

July 21, 2022

## Abstract

*Due to its fast retrieval and storage efficiency capabilities, hashing has been widely used in nearest neighbor retrieval tasks. By using deep learning based techniques, hashing can outperform non-learning based hashing in many applications. However, there are some limitations to previous learning based hashing methods (e.g., the learned hash codes are not discriminative due to the hashing methods being unable to discover rich semantic information and the training strategy having difficulty optimizing the discrete binary codes). In this paper, we propose a novel learning based hashing method, named Asymmetric Deep Semantic Quantization (ADSQ). ADSQ is implemented using three stream frameworks, which consists of one LabelNet and two ImgNets. The LabelNet leverages three fully-connected layers, which is used to capture rich semantic information between image pairs. For the two ImgNets, they each adopt the same convolutional neural network structure, but with different weights (i.e., asymmetric convolutional neural networks). The two ImgNets are used to generate discriminative compact hash codes. Specifically, the function of the LabelNet is to capture rich semantic information that is used to guide the two ImgNets in minimizing the gap between the real-continuous features and discrete binary codes. By doing this, ADSQ can make full use of the most critical semantic information to guide the feature learning process and consider the consistency of the common semantic space and Hamming space. Results from our experiments demonstrate that ADSQ can generate high discriminative compact hash codes and it outperforms current state-of-the-art methods on three benchmark datasets, CIFAR-10, NUS-WIDE, and ImageNet.*

## I. INTRODUCTION

Over the last decade, the amount of image data available has increased exponentially. Finding ways to efficiently store and quickly search through this data has become a major challenge. Among all Nearest Neighbor Search (NNS) [1] methods, hashing has been of considerable interest in many real world applications in the image retrieval field due to its speedy search capabilities and low

storage cost. In general, the hashing technique works by mapping the original high-dimensional features into a common binary representation (i.e., hash code) through a linear or nonlinear mapping function, and an efficient image retrieval task can be accomplished by a few computations at Hamming distance (i.e., the hashing technique may only use several MBytes of storage space to store several GBytes images or several TBytes videos). With the binary representation, the search speed for the data can be remarkably improved and the storage cost dramatically reduced. As a result of this, hashing techniques have become a popular tool for many image retrieval [2–6] and text-image cross-model retrieval tasks [7, 8].

Hashing methods can be divided into two categories: data-independent hashing methods and data-dependent hashing methods. Data-independent hashing methods adopt random projections as hash functions to map the

\*Corresponding author. This work was supported in part by the Key Technology R&D Program of Hunan Province (2018GK2052) and the Science and Technology Plan of Hunan (2016TP1003).

<sup>†</sup>©2019 IEEE. Personal use of this material is permitted. Permission from IEEE must be obtained for all other uses, in any current or future media, including reprinting/republishing this material for advertising or promotional purposes, creating new collective works, for resale or redistribution to servers or lists, or reuse of any copyrighted component of this work in other works. See [http://www.ieee.org/publications\\_standards/publications/rights/index.html](http://www.ieee.org/publications_standards/publications/rights/index.html) for more information

data points from the original high-dimension representation space into a low-dimension representation space (i.e., binary codes). In other words, data-independent hashing methods define a function that is not dependent on the data itself. Existing data-independent hashing methods include Spectral Hashing (SH) [9], and Kernelized Locality-Sensitive Hashing (KLSH) [10]. Unfortunately, data-independent hashing methods need long hash codes to achieve satisfactory retrieval performance. In order to solve the limitation of data-independent hashing methods, recent works have shown that data-dependent hashing methods can achieve better performance with shorter hash codes. Data-dependent hashing methods, which can be further categorized into supervised and unsupervised methods, learn the hash function from training data points. Unsupervised methods are primarily measured by the use of distance metrics (e.g., Euclidean distance or cosine distance) of data point features, including isotropic hashing [11], Discrete Graph Hashing (DGH) [12], Iterative Quantization (ITQ) [13] *et al.* Therefore, in order to bridge the semantic gap, unlike the unsupervised hashing methods, supervised hashing methods utilize the semantic labels to boost the hash function quality. Many researchers have demonstrated that semantic information can improve the quality of hash codes and achieve some success along this direction, e.g., Supervised Hashing with Kernels (KSH) [14], Distortion Minimization Hashing (DMS) [6], Minimal Loss Hashing (MLS) [15], Order Preserving Hashing (OPH) [16], Column Sampling based DIScrete Supervised Hashing (COSDISH) [17], Supervised DIScrete Hashing (SDH) [18]. However, the quality of hash codes generated is highly dependent on the way feature selection is done, and these methods use hand-crafted features for representation. The need to perform manual feature selection has been a big limitation to the success of these methods.

Recently, Deep Neural Networks (DNNs), especially Convolutional Neural Networks (CNNs) have been widely used in the computer vision field [19] and have shown their powerful feature extraction capabilities. Inspired by this, some learning based hashing methods [20–23] that adopt convolutional neural networks as the nonlinear hashing functions to enable end-to-end learning of learnable representations and hash codes, have demonstrated satisfactory retrieval performance on many benchmark datasets. Despite recent learning based hashing methods (as shown in Figure 1) achiev-

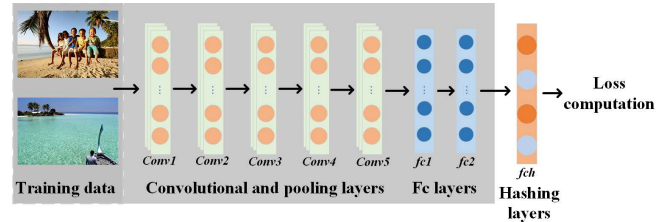


Figure 1: The basic architecture of supervised learning based hashing. (Best viewed in color.)

ing significant progress in image retrieval, there are still some limitations to their usage, e.g., the label information is a simple construction of the similarity matrix, and does not make full use of the multiple label information of the data points [24]. Taking the NUS-WIDE dataset as an example, there is an instance that is annotated with multiple labels, such as “person”, “tree” and “sea”, which can provide abundant semantic information and perfect similar relationship. As described in [25], a method named Deep Joint Semantic-Embedding Hashing (DSEH) that makes full use of multiple label information was proposed. This method can exploit the learned semantic correlation and hash codes in *LabNet* as supervised information and transfer them to *ImgNet* with the form of two constraints. However, there are still two limitations that should be addressed. Firstly, the real-continuous values will be converted by a relaxation scheme to the compact binary code is a mixed-integer optimization problem results in an NP-hard optimization problem. To solve this issue, DSEH addresses the problem by quantizing the real-continuous values to compact binary values, which will cause a large quantization loss. Secondly, another limitation of the DSEH is that it cannot capture the relative similarity between an image pair, i.e., a pair of images should not be seen as **completely** similar or dissimilar. Therefore, using two different networks (same structure with different weights) to train an image pair is often more robust than using a single network.

To solve the above-mentioned challenges, this paper presents **Asymmetric Deep Semantic Quantization (ADSQ)** for efficient and effective image retrieval, which introduces a novel asymmetric training strategy for quantization, offering superior retrieval performance.

The contributions of this work are summarized as follows:

1. We develop a novel asymmetric framework for im-

age retrieval, consisting of two ImgNets and one LabelNet. Two convolutional neural networks (i.e., ImgNets) are trained as different hash functions to compact binary codes for image pairs, and one fully-connected network (i.e., LabelNet) to capture abundant semantic correlation information from the image pair. The model effectively captures similarity relationships between the real-continuous features and binary hash codes, and can generate the discriminative compact hash codes.

2. Binary hash codes of training data points are learned with an iterative optimization strategy. Furthermore, based on the optimization scheme, an asymmetric loss between the binary-like codes and the learned discrete hash codes are imposed to reduce the quantization error.
3. Results from our experiments demonstrate that **ADSQ** outperforms several state-of-the-art methods for the image retrieval.

The remainder of this paper is structured as follows. In Section II, we briefly introduce the related works on learning based hashing quantization. In Section III, we formulate the problem and provide the details of the proposed training strategy. Section IV shows the experimental results and Section V concludes this paper.

## II. RELATED WORK

By representing images as binary codes and taking advantage of fast query retrieval, the use of hashing techniques in image retrieval has attracted considerable attention. Wang *et al.* [26] have provided a comprehensive literature survey that covers the most important methods and latest advances in information retrieval.

According to previous research, hashing methods can be roughly divided into two categories: data-independent and data-dependent methods. Locality Sensitive Hashing (LSH) was one of the data-independent methods used. LSH aims to use several random projections such as hash functions to map the data points into a Hamming space [27]. Some variants of LSH (e.g., kernel LSH [28] and  $p$ -norm LSH [29]) are embedded to extend LSH for performance improvement. However, there are many limitations of using data-independent methods, e.g., the efficiency is low and it requires longer hash codes to attain high performance.

In order to solve the limitations of the data independent methods, the data-dependent methods attains more compact hash codes by combining dataset to achieve a better retrieval accuracy. Data dependent methods can be further categorized into supervised and unsupervised methods. Unsupervised hashing methods learn hash functions that encode data points to binary codes by training from unlabeled data. Typical learning criteria include minimize reconstruction error [13, 30–32], graph based hashing [33, 34], and minimize quantization error [35]. Supervised methods utilize the semantic labels or relevance information to improve the quality of hash codes. For example, Supervised Hashing with Kernels (KSH) [14] and Supervised Discrete Hashing (SDH) [18] generate binary hash codes by minimizing the Hamming distances across similar pairs of data points. Distortion Minimization Hashing (DMS) [6], Minimal Loss Hashing (MLH) [15], and Order Preserving Hashing (OPH) [16] learn hash codes by minimizing the triplet loss based on similar pairs of data points. However, if the feature distribution of a dataset is complex, the performance of these methods will decrease.

Recently, deep learning techniques have yielded amazing results on many computer vision tasks, this success has attracted the attention of researches of learning based hashing methods. Convolutional Neural Network Hashing (CNNH) is one of the early works that made use of a learning-based hashing method. CNNH utilizes two stages to learn the image features and hash codes. Following this work, many learning-based hashing techniques have been proposed, e.g., Deep Semantic Ranking Hashing (DSRH) [36] which learns the hash functions by preserving semantic similarity between multi-label images. Deep Visual-Semantic Quantization (DVSQ) [2] generates the compact hash codes by optimizing an adaptive margin loss and a visual-semantic quantization loss over multi-networks. Deep Supervised Hashing (DSH) [24] designs a loss function to pull the outputs of similar pairs of images together and pushes the dissimilar ones far away. Its outputs are relaxed to real values to avoid optimizing the non-differentiable loss function in Hamming distance. Network In Network Hashing (NINH) [37] adopts a triplet ranking loss to capture the relative similarities of images. Deep Supervised Discrete Hashing (DSDH) [38] uses both pairwise label and classification information to learn the hash codes under a single stream framework. Deep Joint Semantic-Embedding Hashing (DSEH) [25] exploits the learned

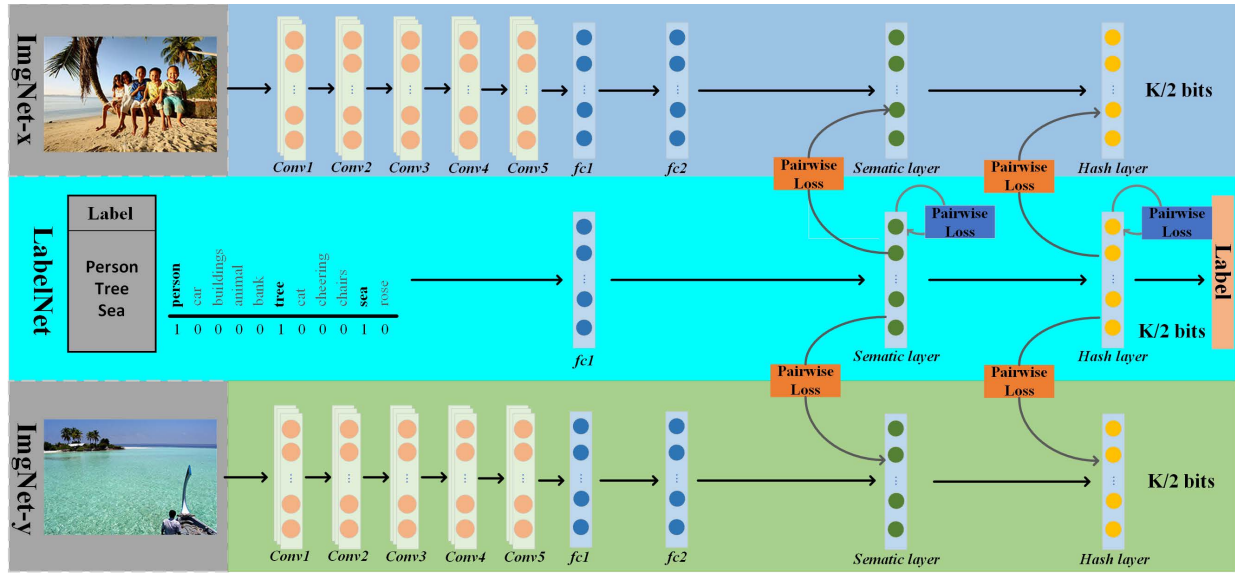


**Figure 2:** The proposed architecture for Asymmetric-Based Deep Semantic Quantization (ADSQ). ADSQ is an end-to-end deep learning framework which adopts two network streams: the first one (LabelNet) with three fully-connected layers (i.e., a common fully-connected layer, a semantic layer, and a hash layer.) is used for rich semantic extraction. The second consists of two asymmetric ImgNets with five convolutional layers and four fully-connected layers (i.e., two common fully-connected layers, a semantic layer, and a hash layer) that are used to generate the discriminative compact hash codes. During the ImgNets training process, we adopt an alternating strategy to learn the parameters of network and binary codes alternately. These codes are both guided by the supervised semantic information and the supervised binary-like representation generated by LabelNet. (Best viewed in color.)

semantic correlation and hash codes in *LabNet* as supervised information and transfers them to *ImgNet* with the form of two constraints.

However, even though DSEH captures abundant semantic correlation to indicate the accurate similarity relationship between samples, it is based on a shallow architecture which cannot effectively differentiate between the real-continuous features and discrete hash codes, because of their high degree of similarity. Therefore, in this paper, we propose a novel learning based hashing method, which can not only capture rich semantic correlation information, but also semantically associate the learned real-continuous features with the binary codes through an asymmetric network.

### III. ASYMMETRIC DEEP SEMANTIC QUANTIZATION

To address the limitations of previous learning based hashing methods, we propose a novel asymmetric learning based method. In order to attain robust image representations, we introduce a method that includes three stream frameworks, i.e., two *ImgNets* and a *LabelNet*. The two *ImgNets* which adopt the same convolutional neural network structure but with different weights, are used to generate discriminative compact hash codes. The *LabelNet*, which captures rich semantic correlation information, is used to guide the two *ImgNets* minimizing the quantization gap. As shown in [39], the top layers of the deep convolutional neural network can gradually extract global and more high-level representations. The details of our model are described in the following subsections.

#### i. Notations and Problem Definition

In this paper, we use boldface uppercase characters like  $\mathbf{B}$  to denote a matrix, and vectors are denoted by boldface lowercase characters like  $\mathbf{b}$ .  $B_{ij}$  means the  $(i, j)$ -th element of  $\mathbf{B}$ .  $\mathbf{B}^T$  is the transpose of  $\mathbf{B}$ , and the  $\ell_2$ -norm of a vector  $\mathbf{b} \in \mathbb{R}^D$  is defined as  $\|\mathbf{b}\|_2 = (\sum_{i=1}^D |b_i|^2)^{1/2}$ . The Frobenius norm of a matrix  $\mathbf{B} \in \mathbb{R}^{m \times n}$  as  $\|\mathbf{B}\|_F^2 = \sum_{i=1}^m \sum_{j=1}^n B_{ij}^2 = \text{tr}[\mathbf{B}^T \mathbf{B}]$ , while  $\text{tr}[\mathbf{B}]$  is the trace of  $\mathbf{B}$  if  $\mathbf{B}$  is square. The symbol  $\otimes$  denotes the element-wise product (i.e., Hadamard product). We use  $\mathbf{1}$  to denote a vector with all elements being 1. In addition, the threshold function  $\text{sign}(\cdot)$  is an

element-wise  $\text{sign}$  function defined as follows:

$$\text{sign}(x) = \begin{cases} 1, & \text{if } x \geq 0 \\ -1, & \text{otherwise} \end{cases} \quad (1)$$

In similarity retrieval systems, we are given a training set  $\mathcal{D} = \{\mathbf{d}_i\}_{i=1}^N$ ,  $\mathbf{d}_i = \{\mathbf{x}_i, \mathbf{y}_i, \mathbf{l}_i\}$ , where  $\mathbf{x}_i \in \mathbb{R}^{1 \times D}$  and  $\mathbf{y}_i \in \mathbb{R}^{1 \times D}$  to denote the feature vector of the  $i$ -th image in the first and second deep convolutional neural networks<sup>1</sup>, respectively.  $\mathbf{l}_i = [l_{i1}, l_{i2}, \dots, l_{ic}]$  are the label annotations assigned to  $\mathbf{d}_i$ , where  $c$  is the number of categories. Furthermore, for supervised learning-based hashing methods, pairwise information can be used which is denoted by  $\mathbf{S} = \{s_{ij}\}^2$ . If  $s_{ij} = 1$ , it means that  $\mathbf{x}_i$  and  $\mathbf{y}_j$  are similar, while  $s_{ij} = 0$  implies that  $\mathbf{x}_i$  and  $\mathbf{y}_j$  are dissimilar. The goal of a learning based hashing method for quantization is to learn a quantizer  $\mathcal{Q} : \mathbf{x} \rightarrow \mathbf{b}_i \in \{-1, 1\}^K$  from an input space  $\mathbb{R}^D$  to Hamming space  $\{-1, 1\}^K$  with a deep neural network, where  $K$  is the length of the binary codes. The similarity labels  $\mathbf{S} = \{s_{ij}\}$  can be constructed from semantic labels of data points or relevance feedback in real retrieval systems.

For a pair of binary hash codes  $\mathbf{b}_i$  and  $\mathbf{b}_j$ , the similar relationship is defined according to a distance metric:  $D(\mathbf{b}_i, \mathbf{b}_j)$ , where  $D(\cdot)$  is a distance metric function (e.g., Hamming distance or cosine distance). In this paper, the aim of our model is to learn two mapping functions  $\mathcal{F}_x$  and  $\mathcal{F}_y$  to map  $\mathbf{X}$  and  $\mathbf{Y}$  into the Hamming space  $\mathbf{B}$ :  $\mathbf{b}_i = \text{sign}(\mathcal{F}_x(\mathbf{x}_i)) \in \mathbb{R}^{K/2}$  and  $\mathbf{b}_j = \text{sign}(\mathcal{F}_y(\mathbf{y}_j)) \in \mathbb{R}^{K/2}$ . For notation simplicity, we denote the length of the hash codes generated by each *ImgNet* from  $K/2$ , as  $K$ . Therefore, the length of the final hash codes is  $2K$ . We define the relationship between their Hamming distance  $\text{Dist}_H$  and inner product  $\langle \cdot, \cdot \rangle$  as follows:  $\text{Dist}_H = \frac{1}{2}(K - \langle \mathbf{b}_i, \mathbf{b}_j \rangle)$ . The larger the inner product of two hash codes, the smaller the Hamming distance, and vice versa. Therefore, the inner product of two hash codes is a reliable criterion for evaluating the similarity between them.

In supervised learning based hashing methods, the Maximum Likelihood (WL) estimation of the hash codes  $\mathbf{B} = [\mathbf{b}_1, \mathbf{b}_2, \dots, \mathbf{b}_N]$  for all  $N$  images is:

$$\log P(\mathbf{S}|\mathbf{B}) = \prod_{s_{ij} \in \mathcal{S}} \log P(s_{ij}|\mathbf{B}), \quad (2)$$

<sup>1</sup>Note that, although we use different symbols  $\mathbf{x}$  and  $\mathbf{y}$  to represent images, both of them denote the same training dataset.

<sup>2</sup>Note that one image may belong to multiple categories.

where  $P(S|B)$  denotes the likelihood function. Given each image pair with their similarity label  $([x_i, y_j], s_{ij})$ ,  $P(s_{ij}|b_i, b_j)$  is the conditional probability of  $s_{ij}$  given the pair of corresponding hash codes  $[b_i, b_j]$ , which is naturally defined as logistic function:

$$P(s_{ij}|b_i, b_j) = \begin{cases} \sigma(\langle b_i, b_j \rangle), & s_{ij} = 1 \\ 1 - \sigma(\langle b_i, b_j \rangle), & s_{ij} = 0 \end{cases} \quad (3)$$

where  $\sigma(x) = 1/(1 + e^{-x})$  is the sigmoid activation function,  $\langle b_i, b_j \rangle = \frac{1}{2}b_i^T b_j$ .

Similar to the hash layer, in the semantic layer, replace two real-continuous features  $r_i$  and  $r_j$  in Eq. 3, the similar information between two real-continuous features can also be used in the same function. Therefore, the similarity probability of  $r_i$  and  $r_j$  can be expressed as likelihood function:

$$P(s_{ij}|r_i, r_j) = \begin{cases} \sigma(\langle r_i, r_j \rangle), & s_{ij} = 1 \\ 1 - \sigma(\langle r_i, r_j \rangle), & s_{ij} = 0 \end{cases} \quad (4)$$

## ii. LabelNet Training

In this section, we have designed an end-to-end fully-connected neural network, named LabelNet, to bridge the semantic information at a more fine-grained level. Given a multiple label vector for instance, LabelNet extracts the semantic features layer by layer. Let  $\mathcal{F}_l(l_i; W_l)$  denote embedding labels for label point  $l_i$ , and  $W_l$  denote the parameters of the LabelNet. Our goal is to maintain the similarity relationship between features and their corresponding hash codes. For LabelNet, the final loss can be defined as follows:

$$\begin{aligned} \min_{W_l} \mathcal{L}^l &= \alpha \mathcal{J}_1 + \beta \mathcal{J}_2 + \gamma \mathcal{J}_3 + \delta \mathcal{J}_4 \\ &= -\alpha \sum_{s_{ij} \in S} (s_{ij} \Lambda_{ij}^l - \log(1 + e^{\Lambda_{ij}^l})) \\ &\quad - \beta \sum_{s_{ij} \in S} (s_{ij} \Theta_{ij}^l - \log(1 + e^{\Theta_{ij}^l})) \\ &\quad + \gamma \sum_{s_{ij} \in S} \|\Omega^l - \mathbf{1}\|_F^2 \\ &\quad + \delta \sum_{i=1}^N \|\tilde{\mathbf{L}} - \mathbf{L}\|_F^2, \end{aligned} \quad (5)$$

where  $\Lambda_{ij}^l = \frac{1}{2}(r_i^l)^T (r_j^l)$ ,  $\Theta_{ij}^l = \frac{1}{2}(\omega_i^l)^T (\omega_j^l)$ .  $r_i^l$  denotes the semantic representation.  $\Omega^l = [\omega_1^l, \omega_2^l, \dots, \omega_i^l]$ ,  $\omega_i^l$

represents the binary-like codes and  $\tilde{\mathbf{L}} = [\tilde{l}_1, \tilde{l}_2, \dots, \tilde{l}_i]$ ,  $\tilde{l}_i = (W^l)^T \omega_i^l + b_i^l$  are the predicted labels of output,  $\mathbf{L}$  is the true label.  $\alpha, \beta, \gamma, \delta$  are hyper-parameters. In (5),  $\mathcal{J}_1$  is used to preserve the similarity relationships in the semantic space, and  $\mathcal{J}_2$  is used to preserve the similarity relationships in Hamming space.  $\mathcal{J}_3$  is the binary regularization (i.e, to promote the hash code discretization), and  $\mathcal{J}_4$  is to maintain the classification loss between the true label and the predicted label.

## iii. ImgNet Training

The image framework of the proposed method is shown in Fig 2. As we can see, we have designed two end-to-end networks, named ImgNet- $x$  and ImgNet- $y$ , respectively, which can map the features of image into binary codes. These ImgNets are guided by LabelNet using the semantic features and the learned hash codes.  $\mathcal{F}_x(x_i, W_x)$  represents the output of the  $i$ -th image in the last layer of the ImgNet- $x$ , where  $W_x$  stands for the parameters of the network. Similarly, we can obtain the output  $\mathcal{F}_y(y_j, W_y)$  corresponding to the  $j$ -th image using the parameters  $W_y$  in the ImgNet- $y$ . To learn the binary codes which can preserve the similarity between image samples and label information, a common practice is to minimize the asymmetric loss between the similarity and the inner product of image-label binary code pairs.

$$\min \|\mathbf{I}^T \mathbf{B}^K - \mathbf{K}\mathbf{S}\|_F^2, \quad (6)$$

where  $\mathbf{I}$  denotes  $\text{sign}(\mathcal{F}_\kappa(\kappa, W_\kappa))$ ,  $\kappa = x, y$ .  $K$  is the length of hash codes.  $\mathbf{S}$  is the pairwise supervised information.

However, there exists a problem for the formulation in (6), it is difficult to implement a back-propagation (BP) algorithm for the gradient with respect to  $\mathbf{I}$  due to their gradients always being zero. Hence, in the paper, we adopt  $\tanh(\cdot)$  to approximate the threshold function  $\text{sign}(\cdot)$ . Thus, Equation (6) is transformed into:

$$\min \|\tilde{\mathbf{I}}^T \mathbf{B}^K - \mathbf{K}\mathbf{S}\|_F^2, \quad (7)$$

where  $\tilde{\mathbf{I}}$  denotes  $\tanh(\mathcal{F}_\kappa(\kappa, W_\kappa))$ ,  $\kappa = x, y$ . For ImgNet,

the final loss can be defined as follows:

$$\begin{aligned}
 \min_{\mathbf{B}^\kappa, W_\kappa} \mathcal{L}^\kappa &= \alpha \mathcal{J}_1 + \beta \mathcal{J}_2 + \eta \mathcal{J}_3 + \nu \mathcal{J}_4 + \mathcal{A} \\
 &= -\alpha \sum_{s_{ij} \in S} (s_{ij} \Lambda_{ij}^\kappa - \log(1 + e^{\Lambda_{ij}^\kappa})) \\
 &\quad - \beta \sum_{s_{ij} \in S} (s_{ij} \Theta_{ij}^\kappa - \log(1 + e^{\Theta_{ij}^\kappa})) \\
 &\quad + \eta \|\tilde{\mathbf{I}} - \mathbf{B}^\kappa\|_F^2 \\
 &\quad + \nu \|\tilde{\mathbf{I}}^T \mathbf{1}\|_F^2 \\
 &\quad + \|\tilde{\mathbf{I}}^T \mathbf{B}^\kappa - \mathbf{KS}\|_F^2 \\
 \text{s.t. } \kappa &= \mathbf{x}, \mathbf{y}, \mathbf{B}^\kappa \in \{-1, +1\}^{n \times K},
 \end{aligned} \tag{8}$$

where  $\Lambda_{ij}^\kappa = \frac{1}{2}(r_i^l)^T(r_j^k)$ , and  $\Theta_{ij}^\kappa = \frac{1}{2}(\omega_i^l)^T(\omega_j^k)$ ,  $r_i^l$  and  $r_j^k$  are semantic representations from LabelNet and ImgNets, respectively.  $\omega^\kappa$  represents the binary-like codes which are obtained by the output of the ImgNets.  $\alpha, \beta, \eta, \nu$  are the hyper-parameters. In (8),  $\mathcal{J}_1$  is used to preserve the similarity relationships between LabelNet and ImgNet in semantic space, and  $\mathcal{J}_2$  is used to preserve the similarity relationships between LabelNet and ImgNet in Hamming Space. (a.k.a.  $\mathcal{J}_1$  and  $\mathcal{J}_2$  exploit the inter-class and intra-class information).  $\mathcal{J}_3$  is the approximation loss between binary-like codes and hash codes. Note that,  $\mathcal{J}_4$  makes a balance for each bit, which encourages the number of negative and positive numbers ( $\pm 1$ ) to be approximately similar among all data points (i.e.,  $\mathcal{J}_4$  is used to maximize the information provided by each bit) [40].  $\mathcal{A}$  is the asymmetric term, this term is used to approximate discrete codes, which measure the image-label similarity information by their inner product.

#### iv. Optimization

In this section, we introduce the training strategy. Firstly, we randomly initialize LabelNet and train it until (5) converges. Secondly, we use the semantic representations and binary-like codes generated by LabelNet to guide the ImgNet training. Finally, the training procedure is repeated for LabelNet and ImgNet until convergence. Here, we only present the training detail for problem (8) since problem (5) can be easily adapted. Hence, we optimize the problem (8) through iterative optimization. Specifically, in each iteration we learn one variable with the other fixed, and so on.

**$W_\kappa$ -step:** Fixing  $\mathbf{B}^\kappa$  to solve  $W_\kappa$ , then the objective

problem can be transformed into:

$$\begin{aligned}
 \min_{W_\kappa} \|\tanh(\mathcal{F}_\kappa(\kappa_i, W_\kappa))^T \mathbf{B}^\kappa - \mathbf{KS}\|_F^2 \\
 - \alpha \sum_{s_{ij} \in S} (s_{ij} \Lambda_{ij}^\kappa - \log(1 + e^{\Lambda_{ij}^\kappa})) \\
 - \beta \sum_{s_{ij} \in S} (s_{ij} \Theta_{ij}^\kappa - \log(1 + e^{\Theta_{ij}^\kappa})) \\
 + \eta \|\tanh(\mathcal{F}_\kappa(\kappa_i, W_\kappa)) - \mathbf{B}^\kappa\|_F^2 \\
 + \nu \|\tanh(\mathcal{F}_\kappa(\kappa_i, W_\kappa))^T \mathbf{1}\|_F^2.
 \end{aligned} \tag{9}$$

Then we use the Back-Propagation (BP) algorithm to update  $W_\kappa$ . For the sake of simplicity, we define  $\mathbf{v}_i = \mathcal{F}_\kappa(\kappa_i, W_\kappa)$  and  $\mathbf{u}_i = \tanh(\mathcal{F}_\kappa(\kappa_i, W_\kappa))$ . Then we can compute the gradient of  $\mathbf{v}_i$  as follows:

$$\begin{aligned}
 \frac{\partial \mathcal{L}^\kappa}{\partial \mathbf{v}_i} &= \left\{ 2 \sum_{s_{ij} \in S} [(b_j^T \mathbf{u}_i - \mathbf{KS}_{ij}) b_j + \frac{\alpha}{2} (\sigma(\Lambda_{ij}) r_j^l - S_{ij} r_j^l) \right. \\
 &\quad \left. + \frac{\beta}{2} (\sigma(\Theta_{ij}) \omega_j^l - S_{ij} \omega_j^l)] + 2\eta(\mathbf{u}_i - b_i) + 2\nu \mathbf{U}^T \mathbf{1} \right\} \\
 &\quad \otimes (1 - \mathbf{u}_i^2),
 \end{aligned} \tag{10}$$

where  $r_j^l$  and  $\omega_j^l$  are semantic representations and Hamming representations generated from LabelNet, respectively.  $\mathbf{U} = [\mathbf{u}_1, \mathbf{u}_2, \dots, \mathbf{u}_i]$ , symbol  $\otimes$  denotes the Hadamard product. After getting the gradient  $\frac{\partial \mathcal{L}^\kappa}{\partial \mathbf{v}_i}$ , the chain rule is used to obtain  $\frac{\partial \mathcal{L}^\kappa}{\partial W_\kappa}$ , and  $W_\kappa$  is updated by using the standard BP algorithm.

**$\mathbf{B}^\kappa$ -step:** Fixing  $W_\kappa$  to solve  $\mathbf{B}^\kappa$ , then the objective problem can be transformed into:

$$\begin{aligned}
 \min_{\mathbf{B}^\kappa} \|\mathbf{U} \mathbf{B}^{\kappa T} - \mathbf{KS}\|_F^2 + \eta (\|\mathbf{U} - \mathbf{B}^\kappa\|_F^2) \\
 \text{s.t. } \mathbf{B}_i^\kappa \in \{-1, +1\}^{n \times K},
 \end{aligned} \tag{11}$$

where  $\mathbf{U} = [\mathbf{u}_1, \mathbf{u}_2, \dots, \mathbf{u}_i]$ , Then (11) can be rewrote as:

$$\begin{aligned}
 \min_{\mathbf{B}^\kappa} \text{tr}[\mathbf{B}^\kappa \mathbf{P}] + \|\mathbf{B}^\kappa \mathbf{U}^T\|_F^2 + c \\
 \text{s.t. } \mathbf{B}_i^\kappa \in \{-1, +1\}^{n \times K},
 \end{aligned} \tag{12}$$

where  $c$  means a constant value and  $\mathbf{P} = -2\mathbf{KS}^T \mathbf{U} - 2\eta \mathbf{U}$ . According to [4], we can update  $\mathbf{B}^\kappa$  bit by bit. In other words, we update one column of  $\mathbf{B}^\kappa$  with other columns fixed. Let  $\mathbf{B}_{*c}^\kappa$  denote the  $c$ -th column and  $\tilde{\mathbf{B}}_c^\kappa$  denote the remaining columns in  $\mathbf{B}^\kappa$ . Let  $\mathbf{U}_{*c}$  denote the  $c$ -th column of  $\mathbf{U}$  and  $\tilde{\mathbf{U}}_c$  denote the matrix of  $\mathbf{U}$  excluding  $\mathbf{U}_{*c}$ . Let  $\mathbf{P}_{*c}$  denote the  $c$ -th column of  $\mathbf{P}$  and

**Algorithm 1** Asymmetric Deep Semantic Quantization (ADSQ).

**Input** Training set  $(X, Y, L)$ ; similarity matrix  $S$ ; hash code length  $K$ .

**Output** Hashing functions  $\mathcal{F}_x$  and  $\mathcal{F}_y$ .

**Initialization** Network parameters:  $W_\kappa, W_l$ , where  $\kappa = x, y$ . Hyper-parameters:  $\alpha, \beta, \gamma, \nu$ , and  $\eta$ . Iteration number:  $T^l, T^v$ . Learning rate:  $\mu$ .

1. **for**  $t = 1 : T^l$  epoch **do**
2. Update  $W_l$  by standard BP algorithm:
3.  $W_l \leftarrow W_l - \mu \nabla_{W_l} \mathcal{L}^l$  according to (5).
4. **end for**
1. **for**  $t = 1 : T^v$  epoch **do**
2. Update  $W_\kappa$ : Fixing  $B^\kappa$  to solve  $W_\kappa$  using standard BP algorithm according to (10),  $\kappa = x, y$ .
3. Update  $B^\kappa$ : Fixing  $W_\kappa$  to solve  $B^\kappa$  according to (14),  $\kappa = x, y$ .
5. **end for**

$\tilde{P}_c$  denote the remaining columns in  $P$ . Then (12) can be rewrote as:

$$\begin{aligned} \min_{B_{*c}^\kappa} \quad & \text{tr}(B_{*c}^\kappa [2U_{*c}^T \tilde{U}_c \tilde{B}_c^{\kappa T} + P_{*c}^T]) + c \\ \text{s.t.} \quad & B^\kappa \in \{-1, +1\}^{n \times K}. \end{aligned} \quad (13)$$

The optimal solution of (13) can be found as follows:

$$B_{*c}^\kappa = -\text{sign}(2\tilde{B}_c^\kappa \tilde{U}_c^T U_{*c} + P_{*c}), \quad (14)$$

Equation (14) can be used repeatedly until all columns are updated.

## v. Out-of-Sample Extension

After our proposed ADSQ model is trained, we can easily generate its hash code through the two asymmetric ImgNets. For example, given a new instance  $x_q \notin \mathcal{X}$ , we directly use it as the input of ADSQ model, each modal only needs to output  $K/2$ -bit hash codes, which are  $b_x^q = \text{sign}(\mathcal{F}_x(x_q, W_x)) \in \mathbb{R}^{K/2}$  and  $b_y^q = \text{sign}(\mathcal{F}_y(x_q, W_y)) \in \mathbb{R}^{K/2}$ , respectively. Therefore, we concatenate the two  $K/2$ -bit binary codes to obtain the final hash codes:

$$b_q = \text{concat}[b_x^q, b_y^q] \in \mathbb{R}^K. \quad (15)$$

## IV. EXPERIMENTS

In order to demonstrate the performance of our proposed ADSQ method, we carried out extensive experiments on three widely used benchmark datasets, i.e., CIFAR-10, NUS-WIDE, and ImageNet, to verify the effectiveness of our method.

### i. Datasets and Settings

**CIFAR-10** [41] dataset consists of 60,000 images with a resolution of  $32 \times 32$  in 10 categories including “truck”, “airplane”, “ship”, “automobile”, “horse”, “bird”, “cat”, “deer”, “frog”, “dog” (each category has 6,000 images). Each image has only one category. In our experiment, we randomly selected 100 images per category (i.e., 1,000 images in total) as the test set, 500 images per category (i.e., 5,000 images in total) as the training set. The rest of the images are used as gallery in the testing phase.

**NUS-WIDE** [42] is a dataset contains 269,648 images collected from the Flickr website. It is a *multi-label* dataset. It contains 81 semantic concepts manually annotated for evaluating retrieval performance. In our experiment, as in [22] and [38], we selected the 21 most frequent concepts. We randomly sampled 100 images per class (i.e., 2,100 images in total) as the test set, 500 images per class (i.e., 10,500 images in total) as the training set. The rest of the images were treated as the gallery in the testing phase. Two images are treated as similar if they share at least a common label. Otherwise, they are considered to be dissimilar.

**ImageNet** [43] dataset is a benchmark dataset for the Large Scale Visual Recognition Challenge (ILSVRC 2015). It contains 1,000 categories with over 1.2M images in the training set and 50,000 images in the validation set, where each image has only one category. As in [4] and [44], we randomly selected 100 categories which led to a database with about 120K images and a query set with about 5,000 images. In this dataset, we randomly selected 100 images per class (i.e., 10,000 in total) as the training set.

### ii. Baselines

We compared our proposed ADSQ method against some traditional and state-of-the-art hashing methods. We roughly divided these methods into two groups: unsupervised hashing methods and supervised hashing methods. The unsupervised hashing methods used



**Table 1:** Configuration of the convolutional layers in *ImgNets* (i.e., *ImgNet-x*, and *ImgNet-y*).

Layer	Configuration				
	Filter Size	Stride	Padding	LRN	Pooling
conv1	$64 \times 11 \times 11$	$4 \times 4$	0	ON	$2 \times 2$
conv2	$256 \times 5 \times 5$	$1 \times 1$	2	ON	$2 \times 2$
conv3	$256 \times 3 \times 3$	$1 \times 1$	1	OFF	-
conv4	$256 \times 3 \times 3$	$1 \times 1$	1	OFF	-
conv5	$256 \times 3 \times 3$	$1 \times 1$	1	OFF	$2 \times 2$

include: **SH** [9], **ITQ** [13], and supervised hashing methods: **SDH** [18], **KSH** [14]. The learning based hashing methods used include **DPSH** [45], **DHN** [21], **CNNH** [22], **DNNH** [37], **DSDH** [38]. The state-of-the-art semantic supervised learning based method chosen was **DSEH** [25]. These methods are based on either AlexNet [39] or CNN-F [46] network architecture. The AlexNet network and CNN-F network have similar network architectures (i.e., They consist of 5 convolutional layers and 2 fully connected layers). As in the traditional hashing methods, we used DeCAF<sub>7</sub> features [47]. For learning-based methods, we used raw images as input. In fact, in the past few years, many more advanced networks have been created such as ResNet [19]. The aim of our paper is to demonstrate a novel technique based on AlexNet that is able to outperform baseline models. If we adopted the advanced networks, we would be unable to know whether the performance gain was given by our **ADSQ** method or by the advanced networks.

We evaluated the image retrieval quality based on the following metrics: Precision-Recall curves (**PR**), mean Average Precision (**mAP**), Precision curves with different Number of top returned samples (**P@N**), Precision curves within Hamming distance 2 (**P@H=2**). For fair comparison, we adopted MAP@1000 for ImageNet and MAP@5000 for other datasets as in [38]

### iii. Implementation Details

The **ADSQ** method was implemented on Pytorch and batch gradient descent was used to train the network. As shown in Figure 2, our model consists of three networks: a LabelNet and two *ImgNets*. We adopt a very famous convolutional neural network, i.e., AlexNet [39] as the two *ImgNets*, and we add two other fully-connected layers (i.e., semantic layer and hash layer) to extract

**Table 2:** Configuration of the fully-connected layers in *ImgNets* (i.e., *ImgNet-x*, and *ImgNet-y*).

Layer	Configuration
full6	4096
full7	4096
Semantic layer	512
Hash layer	$K/2$ -bit hash code

**Table 3:** Configuration of the LabelNet.

Layer	Configuration
full-connected layer	4096
Semantic layer	512
Hash layer	$K/2$ -bit hash code

the semantic feature and project to  $\mathbb{R}^{K/2}$  space, respectively. We fine-tuned convolutional layers and fully-connected layers copied from AlexNet pre-trained on ImageNet and trained the semantic layer and hashing layer by back-propagation (BP). More specifically, the overall model structure contains 5 convolutional layers (i.e., “conv1”-“conv5”) and 4 fully-connected layers (i.e., “full6”-“full7”-“semantic layer”-“hash layer”). The detailed configuration of the 5 convolutional layers is shown in Table 1, where “filter size” denotes the number of convolutional filters. “stride” denotes the convolutional stride. “padding” indicates the number of pixels to add to each size of the input feature. “LRN” denotes whether Local Response Normalization (LRN) [39] is applied or not. “pooling” denotes the down-sampling operation. The configuration of the 4 full-connected layers is shown in Table 2, where the numbers in the table represent the number of nodes in each layer. The LabelNet contains 3 layers, the detailed configuration of the 3 layers is shown in Table 3. In our proposed **ADSQ** method, images in batch form are used as the input and every two images in the same batch constitute an image pair. The parameters of our proposed **ADSQ** model are learned by minimizing the proposed loss function. The training procedure, i.e., **ADSQ**, is summarized in Algorithm 1.

**Network Parameters** In our **ADSQ**, the value of hyper-parameters are  $\alpha = \beta = 1$ ,  $\gamma = 10^{-2}$  and

$\nu = \eta = 10$ . We use mini-batch Stochastic Gradient Descent (SGD) with 0.9 momentum and the learning rate annealing strategy implemented in Pytorch<sup>3</sup>. The mini-batch size chosen was 32 and the weight decay parameter selected was 0.0005.

#### iv. Results and Discussions

Table 4 reports the mAP results on CIFAR-10, NUS-WIDE, and ImageNet dataset, respectively. The length of the hash codes varies from 12 to 48 (i.e., 12, 24, 36, and 48). From the Table 4, it can be observed that the performance of our **ADSQ** achieves the best image retrieval accuracy, and **ADSQ** is better than all baseline methods, including traditional hashing methods, unsupervised hashing methods, supervised hashing methods, and semantic supervised learning based hashing methods. Specifically, Compared to traditional hashing methods, such as, ITQ, the best shallow hashing method using deep features achieves an absolute score more than 78% increase on the mAP performance measure for image retrieval on the CIFAR-10 dataset. Compared to learning based hashing methods, DSDH in particular, the state-of-the-art learning-based hashing method, achieves the best performance among all the learning based methods, our **ADSQ** achieves an absolute score of more than 8% increase on the mAP performance measure. When comparing our **ADSQ** with the semantic supervised learning based hashing method DSEH, it can be seen that **ADSQ** can achieve a more than 3% increase in mAP. On the multi-label dataset NUS-WIDE, compared to the best shallow hashing method, i.e., ITQ, our **ADSQ** achieves score of absolute more than a 40% increase in mAP. Compared to the best learning based hashing method, i.e., DSDH, our **ADSQ** achieves an absolute score of more than a 3% increase in mAP. When compared to the state-of-the-art semantic supervised hashing method, i.e., DSEH, our **ADSQ** achieves an absolute score of more than a 1.5% increase in mAP. On large-scale dataset ImageNet, compared with ITQ, DSDH, and DSEH, our **ADSQ** achieves an absolute score of more than a 20%, 17%, and 8% increase in mAP, respectively. The main difference between our proposed **ADSQ** and DSEH is that our **ADSQ** utilizes semantic information to guide the asymmetric discrete learning procedure but DSEH does not have an asymmetric structure to generate the discriminative compact hash codes. Therefore,

the results demonstrate that the motivation of **ADSQ**, i.e., using semantic information to guide the asymmetric discrete learning procedure can improve image retrieval performance in practical applications. Through in-depth analysis of Table 4, we can find some other insights. **(1)** By comparing KSH, SDH to SH, we can observe that the supervised hashing methods can outperform unsupervised hashing methods because the supervised information can improve performance. **(2)** By comparing DSDH, DPSH, DNNH, CNNH, DHN to SDH, we can find that the learning based hashing methods can significantly outperform the traditional hashing methods. These results demonstrate the advantages of using a deep end-to-end learning structure. **(3)** By comparing semantic supervised learning based hashing methods, i.e., **ADSQ** and DSEH to other baseline hashing methods, we can find that semantic learning based deep hashing can outperform similar learning based deep hashing methods, which means that semantic information is able to learn more optimal binary codes. **(4)** The performance of all methods keep improving with the hash code length increasing.

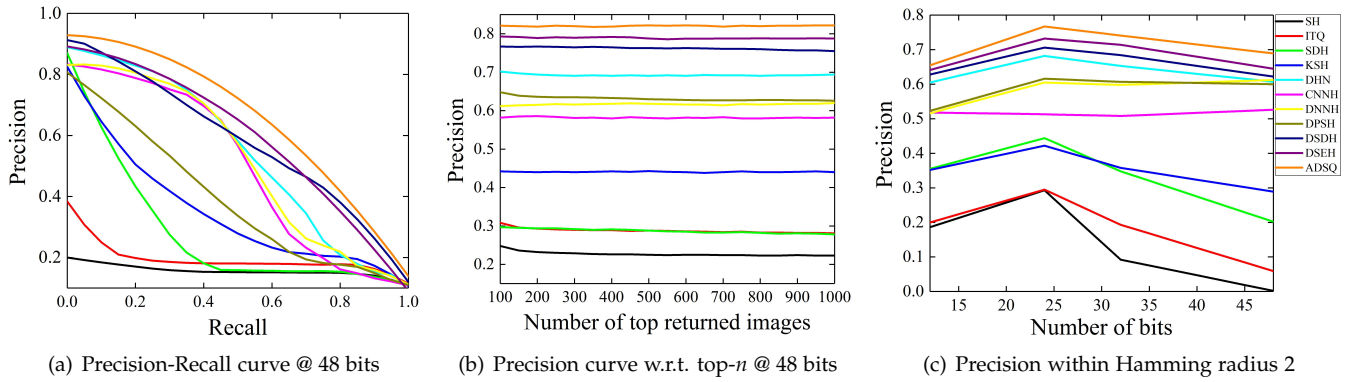
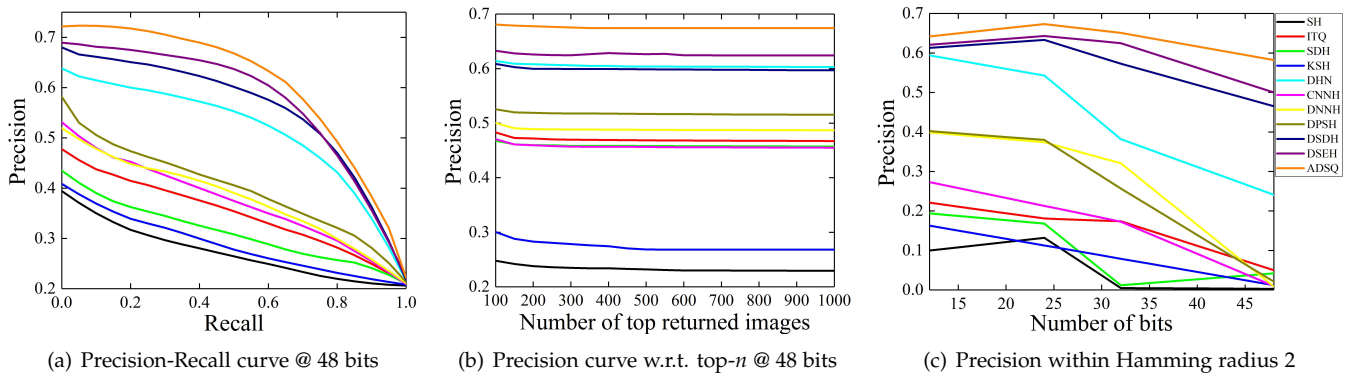
As shown in Figures 3(a), 4(a), 5(a) and Figures 3(b), 4(b), 5(b), experiments were conducted to evaluate the performance by using the metrics of Precision-Recall curves (**PR**) and Precision curves with a different Number of top returned samples (**P@N**), respectively. These metrics are widely used in deploying practical applications. The proposed **ADSQ** significantly outperforms all the baseline methods it was compared. This is very important for image retrieval precision as the primary purpose, where it takes only a small  $N$  to count more on the top- $N$  returned results. This proves the value of the **ADSQ** method in actual image retrieval systems.

The other important indicator is Precision within Hamming radius 2 (**P@H=2**) since it only requires  $O(1)$  time for each query operation. As shown in Figures 3(c), 4(c), and 5(c), **ADSQ** achieves the highest **P@H=2** results on all the datasets with regards to different hash code lengths. This validates the assertion that the proposed **ADSQ** method can attain higher-quality hash codes than all baseline methods and can enable more efficient and accurate Hamming space retrieval. Norouzi *et al.* [48] show that when generating relatively longer hash codes, the Hamming space will become sparse and few data points will fall within the Hamming ball with a radius of 2. This is why many learning based hashing methods

<sup>3</sup><https://pytorch.org/>

**Table 4:** mean Average Precision (mAP) of Hamming Ranking for Different Number of Bits on the Three Image Datasets.

Method	CIFAR-10				NUS-WIDE				ImageNet			
	12 bits	24 bits	32 bits	48 bits	12 bits	24 bits	32 bits	48 bits	12 bits	24 bits	32 bits	48 bits
SH [9]	0.127	0.128	0.126	0.129	0.454	0.406	0.405	0.400	0.185	0.273	0.328	0.395
ITQ [13]	0.162	0.169	0.172	0.175	0.452	0.468	0.472	0.477	0.305	0.363	0.462	0.517
SDH [18]	0.285	0.329	0.341	0.356	0.568	0.600	0.608	0.637	0.253	0.371	0.455	0.525
KSH [14]	0.303	0.337	0.346	0.356	0.556	0.572	0.581	0.588	0.136	0.233	0.298	0.342
DHN [21]	0.555	0.594	0.603	0.621	0.708	0.735	0.748	0.758	0.269	0.363	0.461	0.530
CNNH [22]	0.429	0.511	0.509	0.522	0.611	0.618	0.625	0.608	0.237	0.364	0.450	0.525
DNNH [37]	0.552	0.566	0.558	0.581	0.674	0.697	0.713	0.715	0.219	0.372	0.461	0.530
DPSH [45]	0.713	0.727	0.744	0.757	0.752	0.790	0.794	0.812	0.143	0.268	0.304	0.407
DSDH [38]	0.726	0.762	0.785	0.803	0.743	0.782	0.799	0.816	0.312	0.353	0.481	0.533
DSEH [25]	0.753	0.781	0.807	0.822	0.745	0.785	0.811	0.819	0.449	0.487	0.545	0.576
<b>ADSQ</b>	<b>0.792</b>	<b>0.823</b>	<b>0.836</b>	<b>0.851</b>	<b>0.761</b>	<b>0.793</b>	<b>0.828</b>	<b>0.833</b>	<b>0.493</b>	<b>0.553</b>	<b>0.621</b>	<b>0.649</b>


**Figure 3:** The results of ADSQ and comparison methods on the CIFAR-10 dataset under three evaluation metrics.

**Figure 4:** The results of ADSQ and comparison methods on the NUS-WIDE dataset under three evaluation metrics.

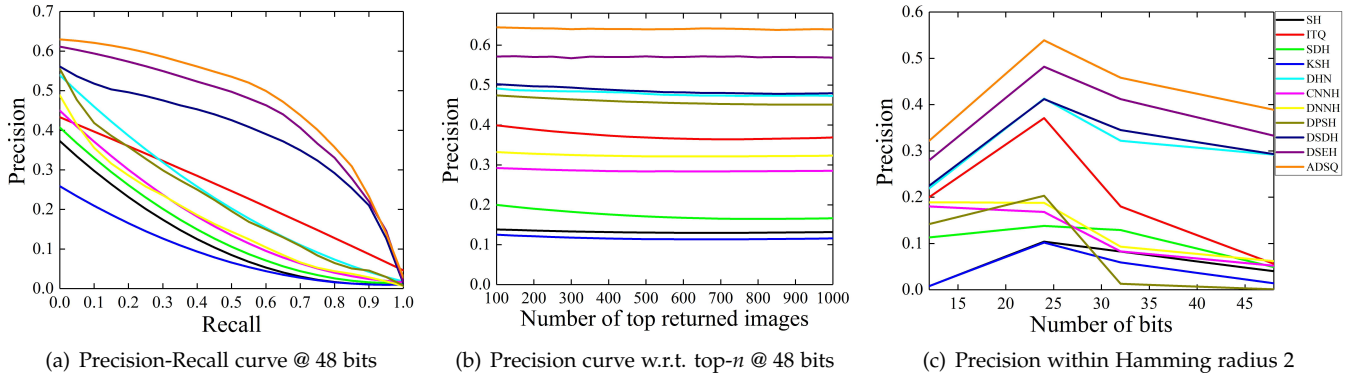


Figure 5: The results of ADSQ and comparison methods on the ImageNet dataset under three evaluation metrics.

can achieve good image retrieval performances on short hash codes.

## v. Discussion

### v.1 Ablation Study

**Necessity of the asymmetric loss term  $\mathcal{A}$  and semantic supervision  $\mathcal{J}_1$  of (8).** In order to demonstrate that the asymmetric loss term and semantic supervision are necessary for ADSQ, we design two variants of ADSQ on the NUS-WIDE dataset. ADSQ- $\mathcal{A}$  denotes (8) without the asymmetric loss term. Therefore, the  $\mathcal{L}_{\mathcal{A}}^{\kappa}$  can be rewritten as  $\mathcal{L}_{\mathcal{A}}^{\kappa} = \alpha\mathcal{J}_1 + \beta\mathcal{J}_2 + \eta\mathcal{J}_3 + \nu\mathcal{J}_4$ . ADSQ- $\mathcal{S}$  denotes (8) without the semantic supervision loss term. Thus, the  $\mathcal{L}_{\mathcal{S}}^{\kappa}$  can be rewritten as to  $\mathcal{L}_{\mathcal{S}}^{\kappa} = \beta\mathcal{J}_2 + \eta\mathcal{J}_3 + \nu\mathcal{J}_4 + \mathcal{A}$ . ADSQ- $\mathcal{AS}$  refers to (8) without both the asymmetric loss term and the semantic supervision. Thus, the  $\mathcal{L}_{\mathcal{AS}}^{\kappa}$  can be rewritten as  $\mathcal{L}_{\mathcal{AS}}^{\kappa} = \beta\mathcal{J}_2 + \eta\mathcal{J}_3 + \nu\mathcal{J}_4$ . The mAP results are shown in Table 5. From Table 5 the following observations were made:

1. ADSQ outperforms ADSQ- $\mathcal{A}$ , ADSQ- $\mathcal{S}$ , and ADSQ- $\mathcal{AS}$  on all cases on NUS-WIDE dataset, which confirms the assertion that the asymmetric loss term  $\mathcal{A}$  and semantic supervision term  $\mathcal{J}_1$  are necessary for ADSQ.
2. The gap between ADSQ and ADSQ- $\mathcal{A}$  is larger than that of ADSQ- $\mathcal{S}$ , this result demonstrates that the asymmetric loss term  $\mathcal{A}$  has a greater impact on ADSQ than the semantic supervision term  $\mathcal{J}_1$ .

Table 5: The mAP results of ablation study of our ADSQ on NUS-WIDE dataset.

Method	12 bits	24 bits	32 bits	48 bits
ADSQ	<b>0.761</b>	<b>0.793</b>	<b>0.828</b>	<b>0.833</b>
ADSQ- $\mathcal{A}$	0.651	0.677	0.729	0.740
ADSQ- $\mathcal{S}$	0.743	0.774	0.811	0.817
ADSQ- $\mathcal{AS}$	0.637	0.651	0.699	0.714

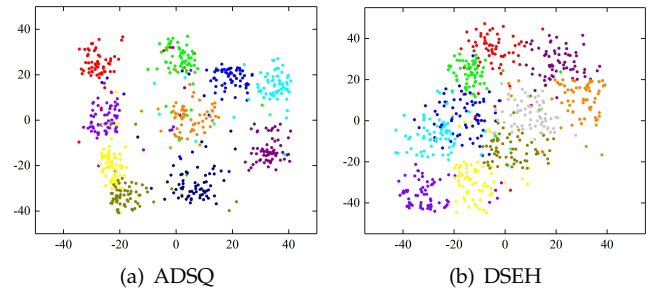
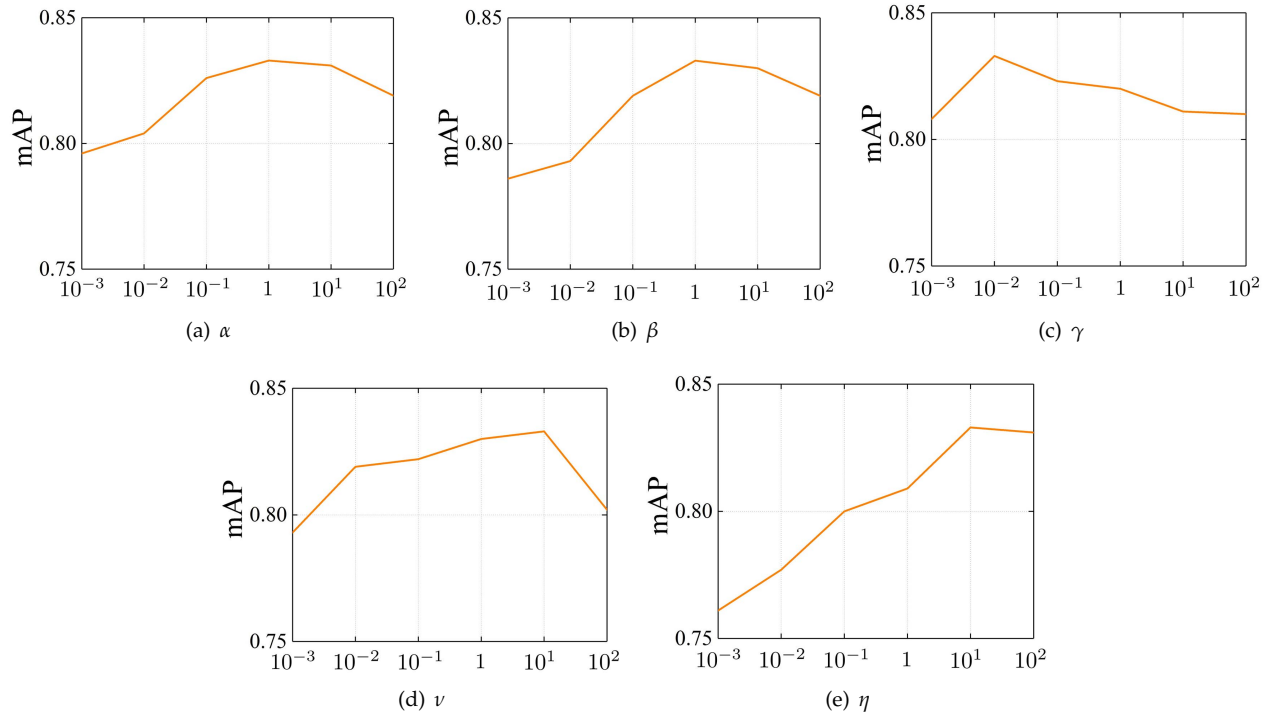


Figure 6: The t-SNE visualization of hash codes learned by ADSQ and DSEH.



**Figure 7:** A sensitivity analysis of the hyper-parameters (i.e.,  $\alpha$ ,  $\beta$ ,  $\gamma$ ,  $\nu$ ,  $\eta$ ).

## v.2 Sensitivity Analysis

In this subsection, we analyze the impact of the hyper-parameters, i.e.,  $\alpha$ ,  $\beta$ ,  $\gamma$ ,  $\nu$ , and  $\eta$ . The experiments are conducted on the NUS-WIDE dataset. We tune a hyper-parameter with others fixed. Specifically, we tune  $\alpha$  by fixing  $\beta = 1$ ,  $\gamma = 10^{-2}$  and  $\nu = \eta = 10$ . Similarly, we fix  $\alpha = 1$ ,  $\gamma = 10^{-2}$  and  $\nu = \eta = 10$  in  $\beta$  tuning and so on. As shown in Figure 7, our model is not affected much by the change of hyper-parameters. This results demonstrate the robustness of our proposed method.

## v.3 Visualization

Figure 6 shows the t-SNE visualization [49] of the hash codes learned by the proposed **ADSQ** method and the state-of-the-art semantic supervised hashing method DSEH on the ImageNet dataset (we sample 10 categories for the case of visualization). We can observe that the hash codes generated by **ADSQ** show clear discriminative distributions where the hash codes in different categories are well separated, while the hash codes generated by DSEH do not show such discriminative structures. The results prove that the hash codes learned

through the proposed **ADSQ** are more discriminative than those learned by DSEH, enabling more effective image retrieval.

## V. CONCLUSION

In this paper, we propose a novel asymmetric semantic learning based hashing method for image retrieval, termed **Asymmetric Deep Semantic Quantization (ADSQ)**. **ADSQ** consists a LabelNet and two asymmetric *ImgNets*, the LabelNet is used to discover semantic information from labels. The two asymmetric *ImgNets* are used to generate their respective discriminative compact hash codes. Moreover, **ADSQ** uses rich semantic information to guide the two *ImgNets* in minimizing the gap between the real-continuous features and discrete binary codes. **ADSQ** is the first asymmetric supervised hashing method which can use abundant semantic information generated by LabelNet to guide the discrete hash codes generation of asymmetric *ImgNets*. Comprehensive experiments on the three benchmark image retrieval datasets demonstrate that **ADSQ** outperforms the state-of-the-art methods. In the future, we will use

two asymmetric networks with different structures to generate high-quality hash codes.

#### ACKNOWLEDGMENT

The authors would also like to thank the associate editor and anonymous reviewers for their comments to improve the paper.

#### REFERENCES

- [1] A. Andoni, "Nearest Neighbor Search in High-dimensional Spaces," in *Proceedings of International Symposium Mathematical Foundations of Computer Science (MFCS)*, Aug. 2011, pp. 1-33.
- [2] Q. Y. Jiang, X. Cui, and W. J. Li, "Deep Discrete Supervised Hashing," *IEEE Trans. Image Processing*, vol. 27, no. 12, pp. 5996-6009, 2018.
- [3] Z. K. Chen, F. M. Zhong, G. Y. Min, Y. L. Leng, and Y. M. Ying, "Supervised Intra- and Inter-Modality Similarity Preserving Hashing for Cross-Modal Retrieval," *IEEE Access*, vol. 6, pp. 27796-27808, 2018.
- [4] Q. Y. Jiang, and W. J. Li, "Asymmetric Deep Supervised Hashing," in *Proceedings of the Conference on Artificial Intelligence (AAAI)*, Feb. 2018, pp. 3342-3349.
- [5] Z. Yang, O. I. Raymond, W. Q. Sun, and J. Long, "Deep Attention-Guided Hashing," *IEEE Access*, vol. 7, pp. 11209-11221, 2019.
- [6] T. T. Yuan, W. H. Deng, and J. N. Hu, "Distortion Minimization Hashing," *IEEE Access*, vol. 5, pp. 23425-23435, 2017.
- [7] C. Deng, Z. J. Chen, X. L. Liu, X. B. Gao, and D. C. Tao, "Triplet-Based Deep Hashing Network for Cross-Modal Retrieval," *IEEE Trans. Image Processing*, vol. 27, no. 8, pp. 3893-3903, 2018.
- [8] H. Liu, M. B. Lin, S. C. Zhang, Y. J. Wu, F. Y. Huang, and R. R. Ji, "Dense Auto-Encoder Hashing for Robust Cross-Modality Retrieval," in *Proceedings of Conference on ACM Multimedia (ACMMM)*, Oct. 2018, pp. 1589-1597.
- [9] Y. Weiss, A. Torralba, and R. Fergus, "Spectral Hashing," in *International Conference on Neural Information Processing (NIPS)*, Dec. 2008, pp. 1753-1760.
- [10] B. Kulis, and K. Grauman, "Kernelized Locality-Sensitive Hashing," *IEEE Trans. Pattern Anal. Mach. Intell.*, vol. 34, no. 6, pp. 1092-1104, 2012.
- [11] W. H. Kong, and W. J. Li, "Isotropic Hashing," in *International Conference on Neural Information Processing (NIPS)*, Dec. 2012, pp. 1655-1663.
- [12] X. S. Shi, F. Y. Xing, K. D. Xu, M. Sapkota, and L. Yang, "Asymmetric Discrete Graph Hashing," in *Proceedings of the Conference on Artificial Intelligence (AAAI)*, Feb. 2017, pp. 2541-2547.
- [13] Y. C. Gong, S. Lazebnik, A. Gordo, and F. Perronnin, "Iterative Quantization: A Procrustean Approach to Learning Binary Codes for Large-Scale Image Retrieval," *IEEE Trans. Pattern Anal. Mach. Intell.*, vol. 35, no. 12, pp. 2916-2929, 2013.
- [14] W. Liu, J. Wang, R. R. Ji, Y. G. Jiang, and S. F. Chang, "Supervised hashing with kernels," in *IEEE Conference on Computer Vision and Pattern Recognition (CVPR)*, Jun. 2012, pp. 2074-2081.
- [15] M. Norouzi, D. J. Fleet, "Minimal Loss Hashing for Compact Binary Codes," in *Proceedings of International Conference on Machine Learning (ICML)*, Jun. 2011, pp. 353-360.
- [16] J. F. Wang, J. D. Wang, N. H. Yu, and S. P. Li, "Order preserving hashing for approximate nearest neighbor search," in *Proceedings of Conference on ACM Multimedia (ACMMM)*, Oct. 2013, pp. 133-142.
- [17] W. C. Kang, W. J. Li, and Z. H. Zhou, "Column Sampling Based Discrete Supervised Hashing," in *Proceedings of the Thirtieth Conference on American Association for Artificial Intelligence (AAAI)*, Feb. 2016, pp. 1230-1236.
- [18] F. Shen, C. H. Shen, W. Liu, and H. T. Shen, "Supervised Discrete Hashing," in *IEEE Conference on Computer Vision and Pattern Recognition (CVPR)*, Jun. 2015, pp. 37-45.
- [19] K. M. He, X. Y. Zhang, S. Q. Ren, and J. Sun, "Deep Residual Learning for Image Recognition," in *IEEE Conference on Computer Vision and Pattern Recognition (CVPR)*, Jun. 2016, pp. 770-778.
- [20] J. Youn, J. Shim, and S. G. Lee, "Efficient Data Stream Clustering With Sliding Windows Based on

- Locality-Sensitive Hashing," *IEEE Access*, vol. 6, pp. 63757-63776, 2018.
- [21] H. Zhu, M. S. Long, J. M. Wang, and Y. Cao, "Deep Hashing Network for Efficient Similarity Retrieval," in *Proceedings of the Thirtieth Conference on American Association for Artificial Intelligence (AAAI)*, Feb. 2016, pp. 2415-2421.
- [22] P. K. Xia, Y. Pan, H. J. Lai, C. Liu, and S. C. Yan, "Supervised Hashing for Image Retrieval via Image Representation Learning," in *Proceedings of the Conference on Artificial Intelligence (AAAI)*, Jul. 2014, pp. 2156-2162.
- [23] J. Wu, Y. He, X. N. Guo, Y. J. Zhang, and N. Zhao, "Heterogeneous Manifold Ranking for Image Retrieval," *IEEE Access*, vol. 5, pp. 16871-16884, 2017.
- [24] H. M. Liu, R. P. Wang, S. G. Shan, and X. L. Chen, "Deep Supervised Hashing for Fast Image Retrieval," in *IEEE Conference on Computer Vision and Pattern Recognition (CVPR)*, Jun. 2016, pp. 2064-2072.
- [25] N. Li, C. Li, C. Deng, X. L. Liu, and G. B. Gao, "Deep Joint Semantic-Embedding Hashing," in *Proceedings of International Joint Conference on Artificial Intelligence (IJCAI)*, Jul. 2018, pp. 2397-2403.
- [26] J. D. Wang, T. Zhang, J. K. Song, N. Sebe, and H. T. Shen, "A Survey on Learning to Hash," *IEEE Trans. Pattern Anal. Mach. Intell.*, vol.40, no.4, pp.769-790, 2018.
- [27] J. Leskovec, A. Rajaraman, and J. D. Ullman, "Mining of Massive Datasets, 2nd Ed," *Cambridge University Press*, 2014.
- [28] B. Kulis and K. Grauman, "Kernelized locality-sensitive hashing," *IEEE Trans. Pattern Anal. Mach. Intell.*, vol. 34, no. 6, pp. 1092-1104, 2012.
- [29] M. Datar, N. Immorlica, P. Indyk, and V.S. Mirrokni, "Locality-sensitive hashing scheme based on p-stable distributions," in *Proceedings of the twentieth annual symposium on Computational geometry*, pp. 253-262, 2004.
- [30] H. Jegou, M. Douze, and C. Schmid, "Product Quantization for Nearest Neighbor Search," *IEEE Trans. Pattern Anal. Mach. Intell.*, vol. 33, no. 1, pp. 117-128, 2011.
- [31] Y. C. Gong and S. Lazebnik, "Iterative quantization: A procrustean approach to learning binary codes," in *IEEE Conference on Computer Vision and Pattern Recognition (CVPR)*, Jun. 2011, pp. 20-25.
- [32] Y. Cao, H. Qi, W. R. Zhou, J. Kato, K. Q. Li, X. L. Liu, X. L. Liu, and J. Gui, "Binary Hashing for Approximate Nearest Neighbor Search on Big Data: A Survey," *IEEE Access*, vol. 6, pp. 2039-2054, 2018.
- [33] Y. Weiss, A. Torralbe, and R. Fergus, "Spectral Hashing," in *In Advances in Neural Information Processing Systems (NIPS)*, Dec. 2008, pp. 1753-1760.
- [34] W. Liu, J. Wang, S. Kumar, and S.F. Chang, "Hashing with Graphs," in *Proceedings of the 28th International Conference on Machine Learning (ICML)*, Jun. 2011, pp. 1-8.
- [35] X. L. Liu, B. Du, C. Deng, M. Liu, and B. Lang, "Structure Sensitive Hashing With Adaptive Product Quantization," *IEEE Trans. Cybernetics*, vol. 46, no. 10, pp. 2252-2264, 2016.
- [36] F. Zhao, Y. Z. Huang, L. Wang, and T. N. Tan, "Deep semantic ranking based hashing for multi-label image retrieval," in *IEEE Conference on Computer Vision and Pattern Recognition (CVPR)*, Jun. 2015, pp.1556-1564.
- [37] H. J. Lai, Y. Pan, Y. Liu, and S. C. Yan, "Simultaneous feature learning and hash coding with deep neural networks," in *IEEE Conference on Computer Vision and Pattern Recognition (CVPR)*, Jun. 2015, pp. 3270-3278.
- [38] Q. Li, Z. N. Sun, R. He, and T. N. Tan, "Deep Supervised Discrete Hashing," in *International Conference on Neural Information Processing (NIPS)*, Dec. 2017, pp. 2479-2488.
- [39] A. Krizhevsky, I. Sutskever, and G. E. Hinton, "ImageNet Classification with Deep Convolutional Neural Networks," in *International Conference on Neural Information Processing (NIPS)*, Dec. 2012, pp. 1106-1114.
- [40] Q. Y. Jiang, and W. J. Li, "Deep Cross-Modal Hashing," in *IEEE Conference on Computer Vision and Pattern Recognition (CVPR)*, Jul. 2017, pp. 3270-3278.

- [41] A. Krizhevsky and G. Hinton, "learning multiple layers of features from tiny images," M.S. thesis, Dept. Comput. Sci., Univ. Toronto, Toronto, ON, Canada, 2009.
- [42] T. S. Chua, J. H. Tang, R. C. Hong, H. J. Li, Z. P. Luo, and Y. T. Zheng, "NUS-WIDE: a real-world web image database from National University of Singapore," in *Proceedings of International Conference on Image and Video Retrieval (CIVR)*, Jul. 2009.
- [43] O. Russakovsky, J. Deng, H. Su, J. Krause, S. Satheesh, S. Ma, Z. H. Huang, A. Karpathy, A. Khosla, M. S. Bernstein, A. C. Berg, and F. F. Li, "ImageNet Large Scale Visual Recognition Challenge," *International Journal of Computer Vision (IJCV)*, vol. 115, no. 3, pp. 211-252, 2015.
- [44] Z. J. Cao, Z. P. Sun, M. S. Long, J. M. Wang, and P. S. Yu, "Deep Priority Hashing," in *Proceedings of Conference on ACM Multimedia (ACMMM)*, Oct. 2018, pp. 1653-1661.
- [45] W. J. Li, S. Wang, and W. C. Kang, "Feature Learning Based Deep Supervised Hashing with Pairwise Labels," in *Proceedings of International Joint Conference on Artificial Intelligence (IJCAI)*, Jul. 2016, pp. 1711-1717.
- [46] K. Chatfield, K. Simonyan, A. Vedaldi, and A. Zisserman, "Return of the Devil in the Details: Delving Deep into Convolutional Nets." [Online]. Available: <https://arxiv.org/abs/1405.3531>
- [47] J. Donahue, Y. Jia, O. Vinyals, J. Hoffman, N. Zhang, E. Tzeng, and T. Darrell, "DeCAF: A Deep Convolutional Activation Feature for Generic Visual Recognition," in *Proceedings of International Conference on Machine Learning (ICML)*, Jun. 2014, pp.647-655.
- [48] M. Norouzi, A. Punjani, and D. J. Fleet, "Fast Exact Search in Hamming Space With Multi-Index Hashing," *IEEE Trans. Pattern Anal. Mach. Intell.*, vol.36, no.6, pp.1107-1119, 2014.
- [49] L. van der Maaten and G. Hinton, "Visualizing high-dimensional data using t-sne," *Journal of Machine Learning Research*, vol. 9, pp. 2579-2605, 2008.